JOURNAL OF FORENSIC SCIENCES

J Forensic Sci, July 2014, Vol. 59, No. 4
doi: 10.1111/1556-4029.12435
Available online at: onlinelibrary.wiley.com

PAPER

CRIMINALISTICS

Laura Ekstrand,[1] *M.S.; Song Zhang,*[1] *Ph.D.; Taylor Grieve,*[1] *B.S.; L. Scott Chumbley,*[1] *Ph.D.; and M. James Kreiser,*[2] *B.S.*

Virtual Tool Mark Generation for Efficient Striation Analysis*,†

ABSTRACT: This study introduces a tool mark analysis approach based upon 3D scans of screwdriver tip and marked plate surfaces at the micrometer scale from an optical microscope. An open-source 3D graphics software package is utilized to simulate the marking process as the projection of the tip's geometry in the direction of tool travel. The edge of this projection becomes a virtual tool mark that is compared to cross-sections of the marked plate geometry using the statistical likelihood algorithm introduced by Chumbley et al. In a study with both sides of six screwdriver tips and 34 corresponding marks, the method distinguished known matches from known nonmatches with zero false-positive matches and two false-negative matches. For matches, it could predict the correct marking angle within ±5–10°. Individual comparisons could be made in seconds on a desktop computer, suggesting that the method could save time for examiners.

KEYWORDS: forensic science, tool mark comparison, computer simulation, screwdriver, statistics, striae

As a result of the recent concerns over the validity of impression evidence analysis, many recent research efforts have focused on improving and reinforcing the scientific basis underpinning firearms and tool mark analysis. Despite vastly varying focuses and approaches, initial studies appear to support the existing conclusions of the forensics community that marks are unique and reproducible. Petraco et al.,(1) for instance, used established numerical pattern recognition algorithms to classify 75 marks in modeling clay from nine screwdrivers with an estimated error of under 3%. Moreover, Bachrach was able to use preliminary 3D scans of bullet surfaces to qualitatively confirm the predicted surface features of the land- and groove-engraved areas of fired bullets (2). Chumbley et al.(3) used a statistical algorithm that compared correlations between subsets of mark profiles from 50 sequentially manufactured screwdriver tips to the correlations resulting from random chance. This algorithm could match screwdrivers to their marks with a 3% false-positive rate, and the results supported the traditional conclusions of tool mark examiners that different screwdrivers, screwdriver sides, and marking angles produce different marks. Research continues to extend and improve these results.

The relative initial success of automated analysis methods suggests that they could be used to streamline and enhance tool mark analysis in new ways. This article investigates the potential of a new tool mark analysis approach based on the statistical matching algorithm introduced in Chumbley et al.(3). This method seeks to link the tool tip directly to the evidence mark through the generation of virtual marks. Both tool tip and evidence mark are digitized using 3D optical profilometry. A computer simulation is used to generate virtual marks from the tip geometry. The algorithm of (3) is used to evaluate the likelihood that a virtual mark is a match with a cross-section selected from the evidence mark. This method has the potential advantage of being able to rapidly generate virtual marks at a large variety of angles and twists and rapidly compare them to the evidence mark. Therefore, it could theoretically be used to exhaustively explore the possible match space and suggest the best matching angle and twist to the examiner. The examiner could then focus his or her traditional analysis on this orientation of the tool, reducing the time required to perform the analysis and helping to ease the burden on backlogged crime labs. This method would also have the benefit of potentially reducing damage to the tool tip caused during the generation of a large number of comparison marks in lead. Finally, as the virtual marks are derived directly from the tip geometry, error rates for the method may be easier to estimate.

This tool-focused approach is relatively new. Bolton-King et al.(4) examined plaster casts of gun barrels but did not relate them to the fired bullets. Geradts et al. suggested relating a scan of the tool tip to the evidence mark in (5) but never implemented that approach. This is likely due to the difficulty experienced in obtaining a 3D scan of the tool tip surface of sufficient accuracy. A profilometer must capture both the microscale surface

[1]Ames Laboratory, Iowa State University, 2096 Black Engineering, Ames, IA 50011.
[2]Illinois State Police Retired, 3112 Sequoia Dr., Springfield, IL 62712.

*Presented at the 65th Annual Meeting of the American Academy of Forensic Sciences, February 18–23, 2013, in Washington, DC; also presented in part at the 42nd AFTE Annual Training Seminar; May 29–June 3, 2011, in Chicago, IL, and in part at the 2011 ASCLD Symposium, September 18–22, 2011, in Denver, CO.

†Supported by Award No. 2009-DN-R-119 from the National Institute of Justice and performed at the Ames Laboratory, which is operated by Iowa State University under contract number DE-AC02-07CH11358 with the U.S. Department of Energy.

Received 7 Feb. 2013; and in revised form 4 June 2013; accepted 8 June 2013.

features that comprise the individual characteristics of the tool and the (typically sharp) macroscale surface curvatures that comprise the class characteristics. Moreover, tool tips are typically metallic and therefore possess high surface reflectivity that produces false features (artifacts) in 3D optical scans. For this reason, this article describes a focus variation process whereby a screwdriver tip can be digitized with sufficient accuracy for the creation of realistic virtual marks.

This article describes the implementation and a preliminary test of this proposed method. A detailed description of the statistical algorithm is not given as it is explained in (3). Both sides of six flat-head screwdriver heads from the set of sequentially manufactured tips used in (3) were digitized and used to generate virtual marks at angular orientations about the edge axis. These were compared to cross-sections from 34 digitized plates marked by the set of screwdrivers at angles to the horizontal of 45°, 60°, and 85°. The results from this test are presented, and they show promise for reliably identifying matches from nonmatches and predicting the angle of the tool mark.

Methods

For this study, six flat-head screwdriver tips were selected from the 50 sequentially manufactured tips used in (3). Tips 2, 3, 4, 5, 8, and 44 were chosen so that the set contained some sequential and some nonsequential tips. Both sides of each tip were used to generate marks in lead. Figure 1 presents the jig used to make 45° marks with these tips. As the figure shows, each tip was fitted into the same screwdriver handle, and this handle was securely fastened to the angled block. The block is constrained to move only along the horizontal (x_{world}). When properly tightened, this assembly allows the user to make an $\alpha = 45°$ mark in lead. For reference, the lead sample used in this jig is *c.* 3.8 cm × 5.1 cm × 0.3 cm. The angled block can be swapped with another to change the value of α. Using this jig, marks were generated on the lead plates for each side of each tip at $\alpha = 45°$, 60°, and 85°. Two of the 45° plates were unavailable at the time of digitization; therefore, this made for a total of 34 marked plates under study.

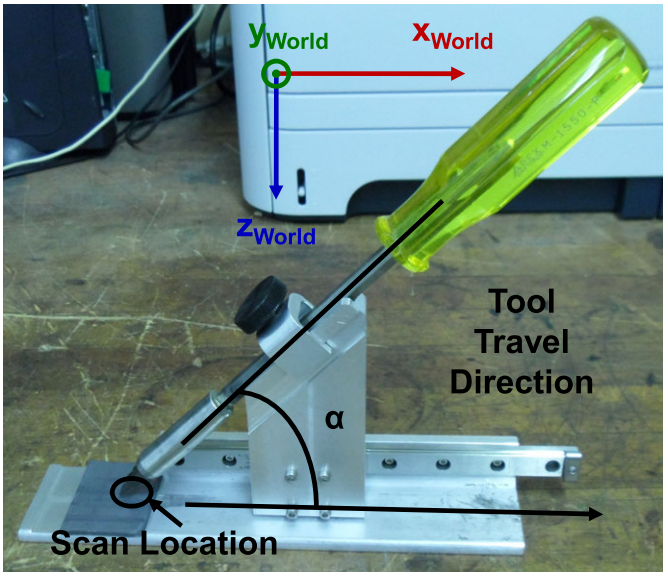

FIG. 1—*Jig for making 45° physical marks.*

Data Collection

Figure 2 presents the Alicona Infinite Focus Microscope (IFM) Model G3 (Alicona Corporation, 1261 Humbracht Circle, Suite G, Bartlett, IL 60103) that was used to digitize both the tips and the marked plates. The IFM uses a technique known as focus variation or depth from focus/defocus to capture the surface geometry (6,7). In any optical system, objects placed at the focal plane are in the sharpest focus. Objects ahead of or behind this plane will be blurred in proportion to their distance from the plane. The Alicona IFM Model G3 uses a vertical translation stage to move the sample in and out of focus. It estimates the depth of a feature based on the translation of the stage and the level of blur in that feature in a 2D image. In this way, it can simultaneously retrieve both the depth and the 2D texture.

The IFM was chosen because of its ability to accurately measure the microscale surface roughness of a screwdriver tip. Several competing screwdriver tip imaging methods were investigated in (8), and the IFM emerged as the only viable option. This is due to the basic operating principle of the focus variation technique. This technique can measure surfaces oriented at up to 85° to the detector (6,7), which allows it to correctly digitize the steep angle of the screwdriver side. Other techniques, such as confocal microscopy, laser profilometry, or stereo vision, have limited numerical apertures or other fundamental limitations that prevent them from accurately imaging shiny metallic surfaces at high angles to the detector. Screwdriver surfaces imaged with these techniques suffer from too many artifacts or too few data points to perform an accurate analysis. Therefore, the IFM was the best choice for this research. Bolton-King et al. found similar results for the steep land-engraving transitions of the NIST standard bullet (7).

Even with the focus variation technique, the resulting digitized tip geometry can contain large numbers of spike artifacts. Figure 3 presents representative tip geometry from the IFM; here, color corresponds to depth. Figure 3(*a*) is tip geometry retrieved from the IFM with no additional lighting in place. The tip is lost amidst the abundance of spike artifacts. An algorithmic procedure (discussed later in Data Preparation) was used to identify and remove the spikes, filling the gaps with interpolated data. The resulting tip is shown in Fig. 3(*b*); while this geometry

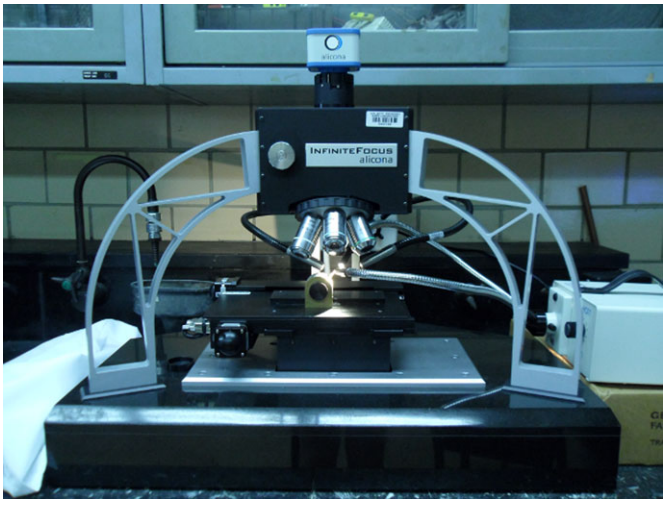

FIG. 2—*The Alicona Infinite Focus Microscope (IFM) Model G3 used in this research.*

resembles a screwdriver tip, it is not as smooth as we might expect. It has strangely "terraced" surfaces that suggest that part of the microscale surface roughness has been lost in the spike removal process. Therefore, it would be desirable to improve the quality of the raw IFM scans.

To prevent the spike artifacts, an improved lighting technique was developed. Two 150 W white light sources are positioned around the IFM, and each is used to power a pair of flexible fiber optic lights. The ends of these cables are carefully and evenly placed about the screwdriver tip as shown in Figs 2 and 4 to brighten the metal tip surface while avoiding the introduction of many specular highlights (glare spots) on the surface. These highlights would cause imaging artifacts. Then, the gamma response of the IFM imaging system is adjusted until the image of the tip surface contains no overexposed (or underexposed) areas. In these areas, the brightness or darkness of the surface is too extreme for the imaging system to correctly detect any surface details. Gamma correction instructs the IFM to respond differently to a spatial change in the level of incoming light; the response becomes nonlinear (curved), so that small changes in light level at the top and bottom ends of the detection range can be resolved. The IFM automatically compensates for this gamma correction to accurately compute the depth. The Alicona color correction tool is also used to ensure that the color response of the sensor is optimal for measuring the depth. These 2D image corrections affect the quality of the depth detection because the focus variation technique relies upon 2D images to compute depth.

After the adjustments to the 2D image, an iterative scanning approach is used to ensure quality. The tip is scanned at 5× magnification and the placement of the light cables is adjusted until the resulting scan is relatively devoid of spike artifacts. When this is satisfied, it is rescanned at 10× magnification to give the final geometry a finer spatial and vertical resolution. Figure 3(*c*) presents a representative result of using this lighting technique. By visual examination, it was determined that the new scanning procedure yielded sufficiently clean geometry except for clusters of spikes at the ends of the tips. As the digitized data is graphical in nature, the best, easiest, and quickest way to evaluate the quality of the data is with a simple visual examination. During this examination, several views are inspected to ensure that the viewer is not fooled by the effects of parallax.

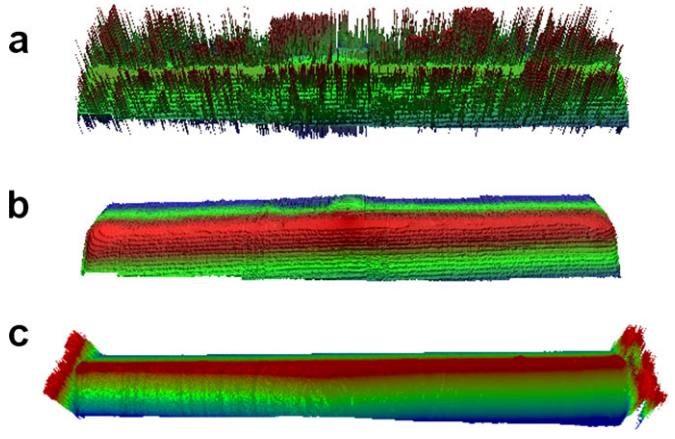

FIG. 3—*Spike noise removal. (a) Tip digitized with no additional lighting. (b) Tip in (a) after algorithmic cleaning. (c) Tip digitized with new lighting procedure, prior to algorithmic cleaning.*

In contrast to the tips, the marked plates have relatively flat geometry and require only a minimal scanning procedure. The additional light from the four fiber optic cables is unnecessary to obtain accurate results, and therefore, their light sources are powered off. Gamma and color adjustments are made, and then, the plate is scanned at 10× magnification. If spikes are present, the gamma and color levels are readjusted and the plate is rescanned at 10× magnification. This is repeated until the plate geometry is accurate. The high magnification can be used for iteration because the geometry is typically correct on the first or second scan.

The final resulting tip and plate scans at the 10× magnification have a spatial resolution of 0.804 μm. The tips and plates for this study were digitized with a depth resolution of 2 μm (the IFM's *low* setting). This setting was experimentally determined to be sufficiently accurate for use with the statistical algorithm and appreciably increased the scanning speed. At the 10× magnification and the low setting, a plate or a tip takes *c.* 25 min to digitize.

Data Preparation

To improve the quality of virtual mark generation and subsequent statistical comparisons, the tips and marked plates require algorithmic cleaning to remove unneeded boundary regions and spike artifacts. Figure 5 presents the tip of 3(*c*) with its 2D texture mapped onto its depth data both before and after algorithmic cleaning. From Fig. 5(*a*), we can see that the spike noise at the ends is dark; the spikes occur where the screwdriver geometry falls sharply away from the IFM detector. As this portion of the geometry is not useful for making virtual marks, we remove it with basic image processing algorithms. Thresholding of the 2D texture and the Alicona-computed quality map is used to remove points that are dark and/or low in quality. The connected components algorithm is then used to identify and keep only the main bulk of the tip geometry.

After the end noise is removed, the aforementioned spike removal algorithm is applied to remove any sharp spike artifacts from the bulk of the tip geometry. First, a seventh-order polynomial is fitted to each column of data. Any point with a depth value 100 μm different from the value predicted by its column's polynomial is removed. This process is repeated with the rows of the data. Finally, small holes are filled by linearly interpolating between the good points at their edges. The threshold value and polynomial order for both the rows and columns were determined by experimentation.

The result of this cleaning for Fig. 5(*a*) is shown in Fig. 5(*b*). The geometry resembles the edge of a screwdriver tip, and the microscale surface roughness has the expected continuous appearance. From a 3D visual examination of the cleaning results for the tip sides, this cleaning procedure was determined to function effectively. When tested on a 3.20 GHz desktop computer, the entire cleaning process takes about 1–2 min.

Figure 6 presents a digitized marked plate before and after algorithmic cleaning. In Fig. 6(*a*), the plate has dark edges with spikes and no striations. These edges are the unmarked parts of the plate. To remove these edges, the plate is first thresholded using the 2D texture and the Alicona quality map in the same manner as the tip geometry. Then, the x and y gradients of the 2D texture are computed and used to locate the edges of the striated portion. Any data points beyond these edges are removed. The depth data is then median filtered to diminish the presence of any spikes in the striations. (Median filtering, unlike Gaussian

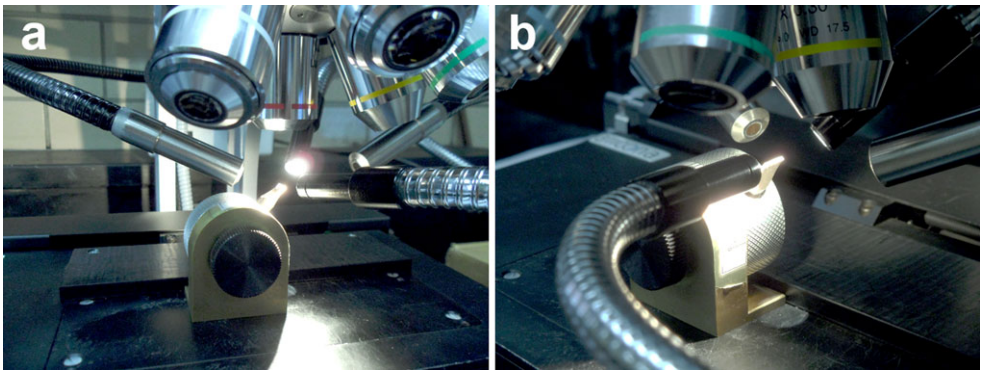

FIG. 4—*Close-ups of the tip lighting in the IFM, showing the four fiber optic cables. (a) Front view. (b) Side view.*

FIG. 5—*Tip 8 Side A with overlaid 2D texture. (a) Before cleaning. (b) After cleaning.*

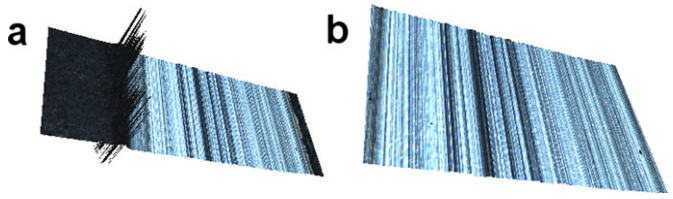

FIG. 6—*Plate marked by Tip 25 Side A at 45° with overlaid 2D texture. (a) Before cleaning. (b) After cleaning.*

filtering, preserves the edges of the striations.) Finally, a detrending operation is performed; a plane is fit to the data and then subtracted from the data. This detrending is a necessary preprocessing step for the statistical comparison algorithm; it corrects for the unavoidable variations in the orientation of the plate during digitization. Comparing Fig. 6(*b*) with (*a*), we can see that the unmarked plate has been successfully removed and the striation surfaces have the expected smoothness and continuity. A 3D visual examination of the cleaned plates was performed to ensure that the plate edges were correctly removed using this procedure. Much like this process for the tip geometry, this cleaning process takes about 1–2 min on a 3.20 GHz desktop computer.

Virtual Tool Mark Generation

Figure 7 illustrates the process of making a mark. The screwdriver is oriented at some angle to the horizontal and given a slight twist of angle β about the handle. The inset shows the surfaces of one side of the screwdriver tip in contact with the plate (the part of the tip that we have digitized). The black line represents the points that have the maximum depth on the tip geometry as it is currently oriented. These points should dig the deepest into the plate and therefore be responsible for leaving the striations. As the tip moves across the plate, the mark cross-section perpendicular to the direction of tool travel is the black line projected onto that same perpendicular direction. Indeed, we could find this profile by "squishing" the tip geometry between two planes, each oriented perpendicular to the direction of tool travel. After this squishing process (a geometric projection of the tool tip geometry), the points in the black line would be the same as the mark cross-section, and they would constitute the bottom edge of the flattened screwdriver tip. If we could measure along this edge with a stylus profilometer, we could predict the striations of the mark without ever generating a physical mark.

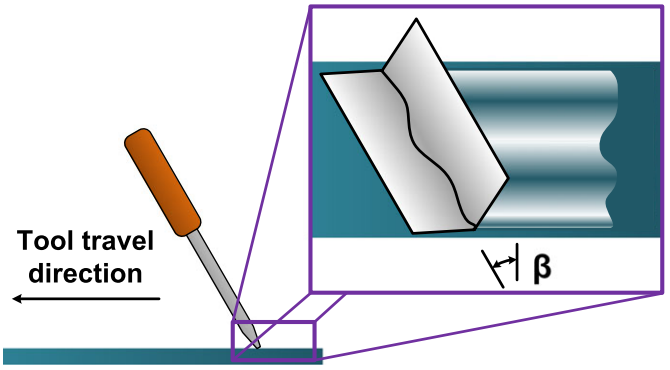

FIG. 7—*The tool mark as a projection of the tool tip geometry.*

This idea of projecting the tool tip geometry along the direction of tool travel and retrieving the mark cross-section from the bottom of the flattened tip forms the basis of the tool mark simulation employed in this study. This simulation is a first approximation, and as such, it ignores the effects of material properties, forces, deformations, and the possibility of partial markings, as these effects are difficult to model. The geometry of the tip is assumed to transfer completely to the plate.

Efficiently implementing this process in the computer requires the use of computer graphics software. Each tip used in this research contains millions of points. Each point can be uniquely described by its x, y, and z values. To simulate the mark, each point must be moved into the desired marking position and then projected onto the perpendicular. This can be performed by multiplying its position values (arranged in a vector) by a matrix; this conservatively requires nine multiplication and six addition operations for each point. The computer's central processing unit would have to perform each matrix multiplication one at a time,

and these small computations would add up to a large load that would take a long time. An exhaustive search through the points would then have to be conducted to determine which of them fell along the edge that produces striations. Finally, linear interpolation between the points would be required to resample the edge with the appropriate resolution to correctly compare it with a cross-section from the marked plate. Therefore, performing these computations on the CPU could take a very long time.

Nevertheless, the mark simulation is a computer graphics problem, and therefore, we can use a computer graphics library (such as OpenGL or Direct3D) to accelerate and simplify its solution. Computer graphics libraries provide easy access to the computer's graphics processing unit (GPU). The GPU consists of a set of small processors known as shader processors (9). Each shader processor can perform its own independent computations. This allows the GPU to process several points simultaneously, greatly reducing the amount of time required for the matrix multiplication process. A computer graphics library also provides tools to simplify finding the edge of the flattened screwdriver and resampling this edge. For this research, we chose to use OpenGL as our graphics library as it is freely available on the vast majority of desktops and laptops and runs under almost every operating system.

Figure 8 presents a simple analogy of how OpenGL and other computer graphics libraries work. The user defines a 3D object by giving OpenGL its x, y, and z values and positions and orients it in the scene by directing OpenGL to multiply it by a series of translation and rotation matrices. Likewise, the user positions a simulated camera in the scene. OpenGL simulates the process of taking a picture of the scene by multiplying the points of the object by a projection matrix to flatten them. Then, it resamples this image of the scene so that the new points are arranged precisely in a rectangular grid. This results in a 2D picture of the scene that can be displayed on the user's computer screen. Because the depth of the points in the scene are perfectly known (they were given by the user), the camera can also produce a rectangularly sampled depth image, which is a 2D array of the depth values of the points closest to the camera.

To simulate the marking process using OpenGL, we defined the x-axis of the scene as the direction of tool travel and then placed the screwdriver in the scene with the edge at the desired orientation to this direction. The screwdriver points are then multiplied by a simple projection matrix that flattens the geometry in the direction of tool travel. The resulting flattened geometry is extruded so that the camera can see it. This is performed using two copies of the flattened geometry and directing OpenGL to draw triangles between them as they are pulled apart (a process analogous to a game of cat's cradle). The camera is then used to take a resampled depth image of this scene to retrieve the edge of the flattened tip. This edge is the simulated mark.

Figure 9 shows a representative virtual tool mark made using this process. The mark has very steep sides which arise from the edges of the screwdriver tip geometry. These are not useful for the comparison and may confuse the comparison algorithm, so they are cut off. A trimming algorithm was developed to recommend a cutting location to the user. This algorithm computes the mean and standard deviation of the virtual mark, and then, moving in from the first and last points of the mark, finds the first pair of points that have values within one standard deviation of the mean. The algorithm then repeats the process on the data lying between this new pair of start and end points to find a second pair of start and end points that are closer together. The sides of the box in Fig. 9 are these recommended points for trimming. Although the software user has the option to manually change these points, for this research, the autogenerated points were used for trimming as they were found to be reasonable through a visual examination. The entire virtual marking process, including the trimming suggestion, takes on the order of ten seconds on a 3.20 GHz desktop computer with a midrange graphics card intended for CAD applications.

Results and Discussion

Virtual Mark Verification

To validate the ability of the tool mark simulator to faithfully reproduce a mark from the tool tip geometry, three sets of artificial tool tip data were generated from standard geometric functions and used to generate virtual marks. Figure 10 presents the cross-sections of these geometric functions compared with their virtual marks. The cross-section of each tool was generated from 2000 samples of the geometric function (triangle, semicircle, or trapezoid). This profile was copied 1000 times to form an extruded tool which was then placed in the simulation scene with the plane of the geometric cross-section perpendicular to the direction of tool travel.

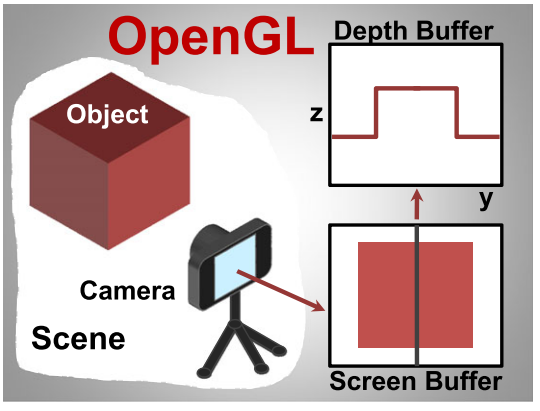

FIG. 8—*OpenGL simulates the process of taking a picture. As the depths of the points on the cube are known, OpenGL can take a "depth" image of the scene.*

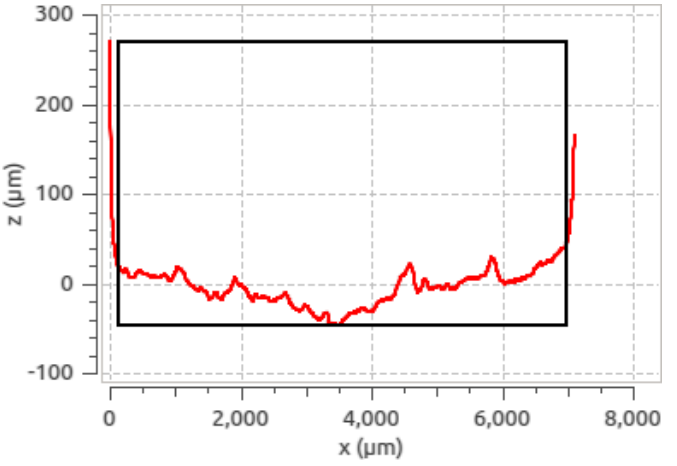

FIG. 9—*A virtual tool mark. The left and right edges of the box denote the trim points that the software has suggested to the user.*

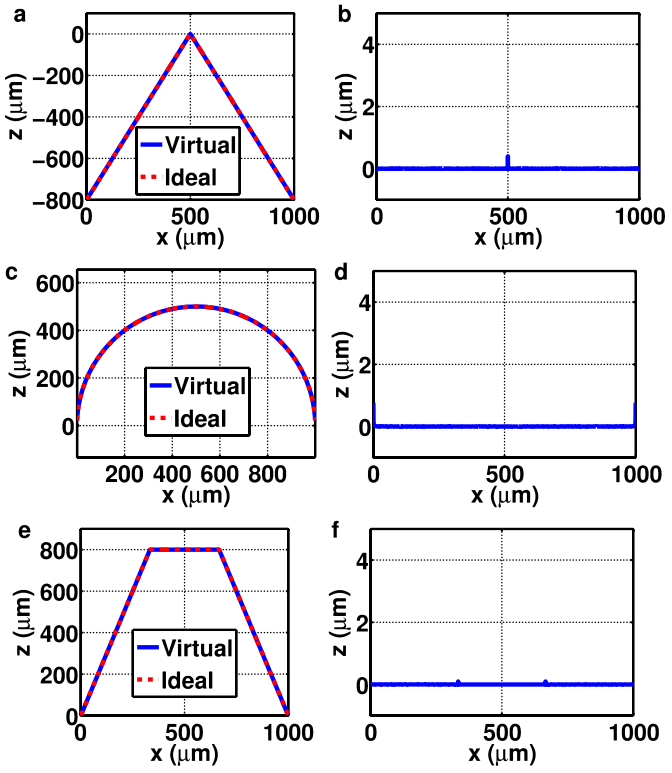

FIG. 10—*Comparisons of geometric standard tools to their virtual marks. (a) Triangle function. (c) Semicircle function. (e) Trapezoid function. (b), (d), (f) Errors for (a), (c), and (e), respectively.*

Due to the nature of the resampling process in OpenGL, the resulting virtual mark could not be directly compared with the original tool cross-section. Although the virtual marking simulation samples the edge at the same resolution as the underlying tool data, the camera may not be perfectly aligned with the tool data. Therefore, there is some offset in where the sampling occurs along the geometric function. To correct for this, the inverse function of the geometric cross-section was applied to the virtual mark and the offset estimated as the median of the errors between the sample locations. The geometric function was then sampled with this offset and compared with the virtual mark.

The resulting root mean square errors were 0.0011%, 0.0055%, and 0.0004% for the triangle, semicircle, and trapezoid, respectively. These errors are negligible for the application of comparing tool marks. Moreover, they agree with similar results for 2D OpenGL resampling found in (10). Therefore, the algorithm is judged to accurately reproduce the geometry.

Visual inspections of the virtual marks also seem to reinforce the validity of the tool mark simulation. Figure 11 presents a representative visual comparison between a physical mark and a known matching virtual mark. Both of these marks were made with the same side of the same tip at an angle of 45°. As the figure shows, while the two profiles have minor differences, the visual resemblance is uncanny. Many of the features have been transferred faithfully from the tip to the plate. Nevertheless, there is some minor spike noise present on the digitized tip that has entered the virtual mark.

Statistical Results

To evaluate whether the proposed method shows promise for reliably matching an evidence mark to the tool tip that created it, a small statistical study was carried out. Each side of each of the six screwdriver tips was used to generate virtual tool marks in increments of 5° beginning at 30° and ending at 90°. Each virtual mark was then compared to the middle cross-section of each marked plate using the statistical algorithm from (3). In the interests of better lighting, some of the plates were digitized in the reverse direction; therefore, the virtual marks were also flipped left to right and compared to the marked plates.

For this study, known matching virtual marks were defined to be those made by the same side of the same screwdriver tip used to make the physical mark and oriented in the same direction as the scan of the physical mark. The correct orientation of the virtual mark relative to the scan direction of the plate was determined by visual inspection. Known nonmatching virtual marks were defined as those made with a different tip or tip side from that of the physical mark. The assumption was made that different sides of the same tip make their own unique marks because the results of prior studies (such as [3]) have reinforced this assumption. Moreover, known nonmatching virtual marks included those made with the same side of the same tip that had been flipped relative to the scan direction of the marked plate. The flipped virtual marks of the other known nonmatches were also considered known nonmatches.

Known Nonmatches

Figures 12–14 present the averaged T1 statistic values resulting from comparisons between 45°, 60°, and 85° marked plates and known nonmatching virtual marks. T1 values are the measures of match likelihood produced by the algorithm of (3). A T1 value near zero or a negative T1 value indicates a low match likelihood, while a higher positive T1 value suggests a high match likelihood. As part of the algorithm relies on taking random samples from the mark profiles, the T1 values can vary for the same comparison. To reduce this fluctuation, the T1 values used in this study were actually the average of 200 such T1 values for each comparison. In these figures and those that follow, the T1 values are plotted in box plots. The box denotes the middle 50% of the spread, and the dark line represents the median. The whiskers extend from the box to the nearest data points within 1.5 times the length of the box from its upper and lower edges. (Thus, these are standard box plots.) Any points outside of this range are considered outliers and plotted with a circle.

In Figs 12–14, the large majority of the T1 values cluster around zero. As expected, there is no clear relationship between the boxes or medians and the angle of the virtual mark. The lower whiskers fall near -1, and the upper whiskers fall near 1. The large majority of the outliers lie between ± 2.5. Previous experiences with this algorithm (such as the results in [3]) suggest that the outliers between ± 2.5 are reasonable for the functioning of this algorithm. Nevertheless, there are some negative outliers of larger magnitude that cause concern.

A visual examination of the comparisons that yielded negative outliers below -2.5 revealed them to be caused by a weakness in the statistical algorithm. Figure 15 presents one such comparison. Here, the boxes denote the regions within the two profiles with the maximum correlation. The algorithm first locates these regions and then randomly selects a common distance and direction relative to these regions as the location for a pair of validation windows. In the case of Fig. 15, the algorithm does not have many viable choices for this rigid shift. Because the maximum correlation windows are at opposite ends, it cannot choose a distance far to the right or left. To the right, it runs into the

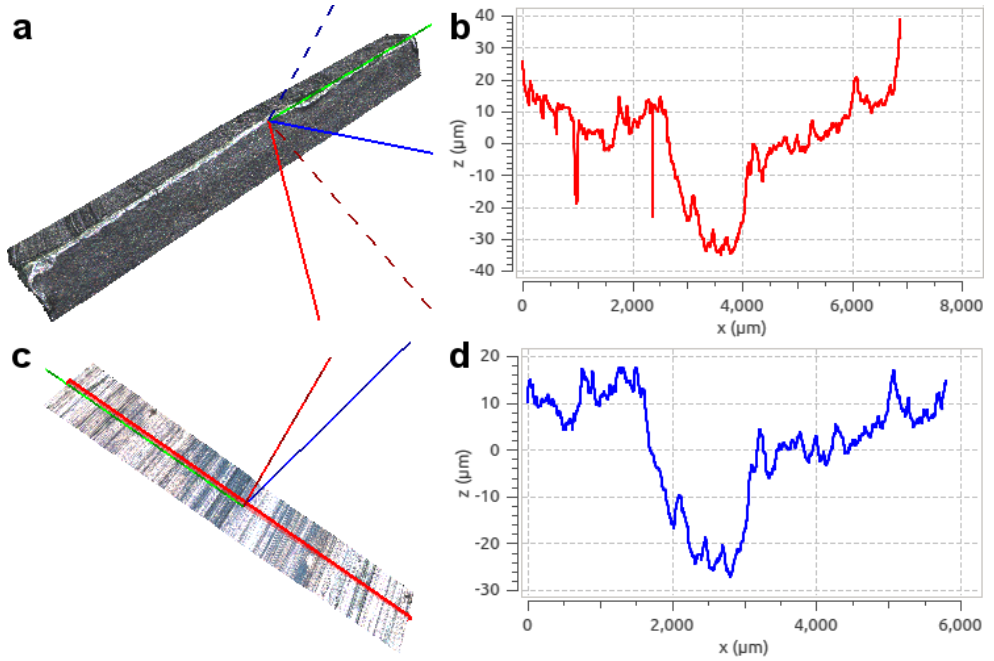

FIG. 11—*Known match comparison. (a) Digitized tip. (b) Virtual mark at 45°. (c) Digitized plate marked at 45°. (d) Middle cross-section of (c).*

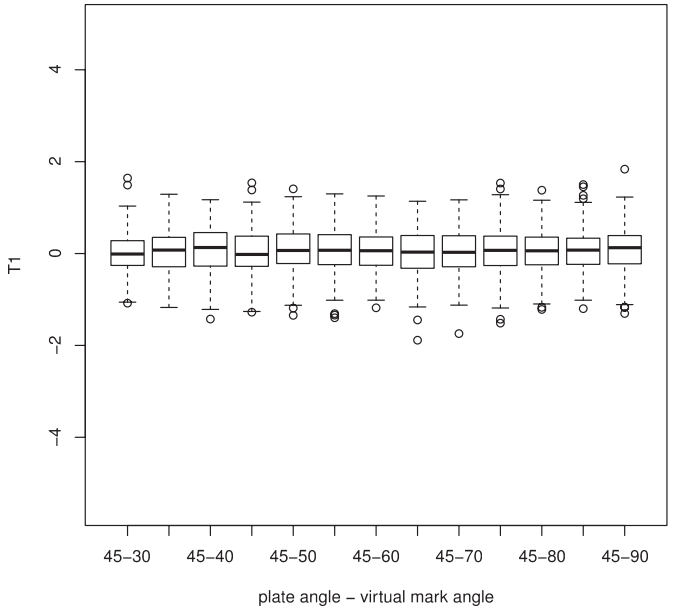

FIG. 12—*Averaged T1 values from statistical comparisons of 45° physical marks to known nonmatching virtual marks.*

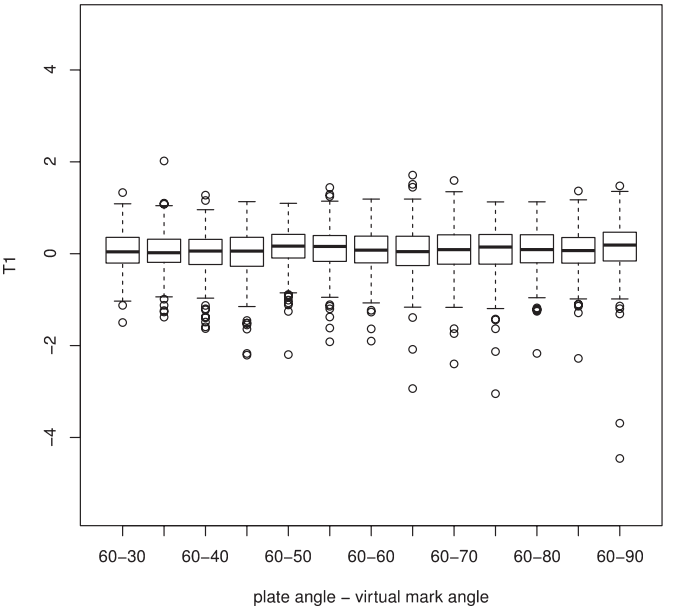

FIG. 13—*Averaged T1 values from statistical comparisons of 60° physical marks to known nonmatching virtual marks.*

end of the virtual mark data, and to the left, it runs into the end of the physical mark data. As there is more data on the right than the left, it will most likely put almost all of its validation window pairs there. In that small region, the virtual mark slopes strongly upward, while the physical mark slopes downward. Because these opposing slopes dominate the rigid shift validation window correlations, the T1 statistic becomes strongly negative. A visual inspection of the other strongly negative comparisons revealed that they were all caused by similar opposite end problems. The opposite end problem could theoretically lead to high positive T1 values and consequently false positives. The results of the study were therefore visually checked to ensure that this opposite end problem was not the source of any false positives or false negatives, and future work will modify the algorithm to prevent this problem.

Known Matches

Figure 16 presents the results for known matches with plates marked at 45°. There is a clear trend in the T1 value distributions as the angle of the virtual mark changes. Above 65°, the values cluster around zero in the same manner as those of a known nonmatch. Below 65°, the distributions rise, peaking near 40° and 45°. At this peak, the distributions are actually very

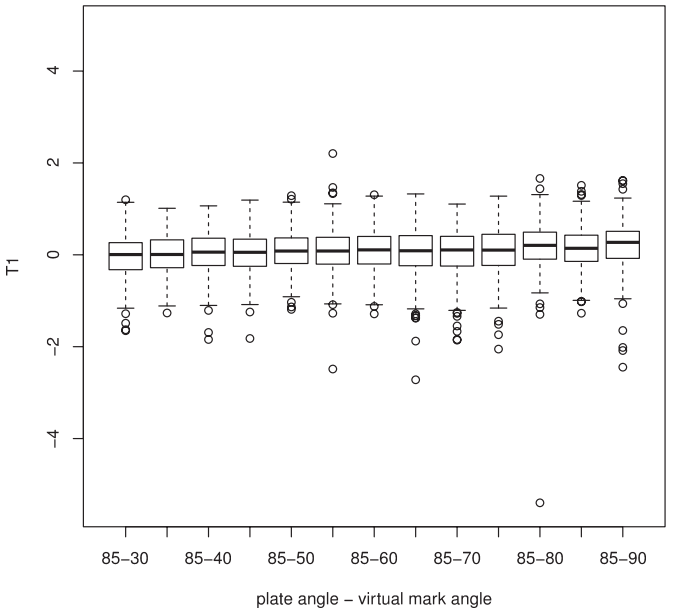

FIG. 14—*Averaged T1 values from statistical comparisons of 85° physical marks to known nonmatching virtual marks.*

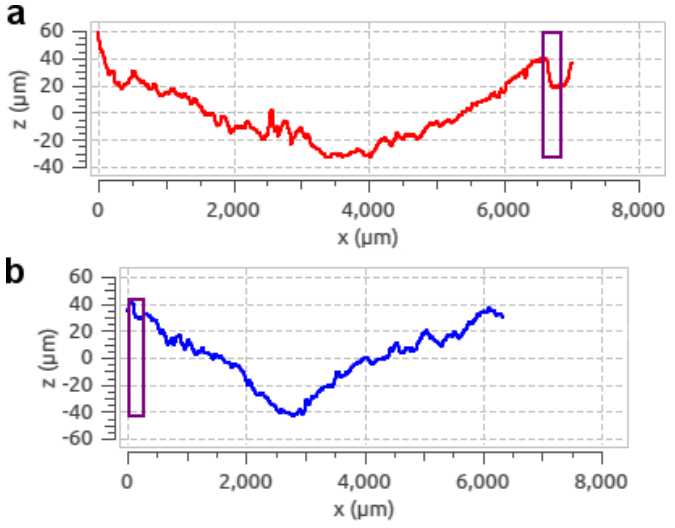

FIG. 15—*A statistical comparison exhibiting the opposite end problem with T1 = −5.39871. (a) Virtual mark. (b) Physical mark.*

tight, and every nonoutlier is well above 2.5. Nevertheless, there are two outliers near zero for 40° and 45°. Upon inspection, the same marked plate, designated P5A-45, was responsible for both of these outliers. Indeed, the T1 values for P5A-45 were below 1.0 for every virtual mark angle.

Figures 17 and 18 present similar results for known match comparisons with plates marked at 60° and 85°, respectively. Like the results for 45°, these results also display clear peaks in the T1 value distributions near the angle of the marked plates. In Fig. 17, the peak is slightly broader and has a few outliers under it. A closer inspection of this data revealed that this is due to different marked plates having slightly different T1 peaks rather than a false nonmatch with a particular plate. In Fig. 18, the peak is narrower; the outliers under this peak are due both to another false nonmatch with P2A-85 and slight differences in the peak locations.

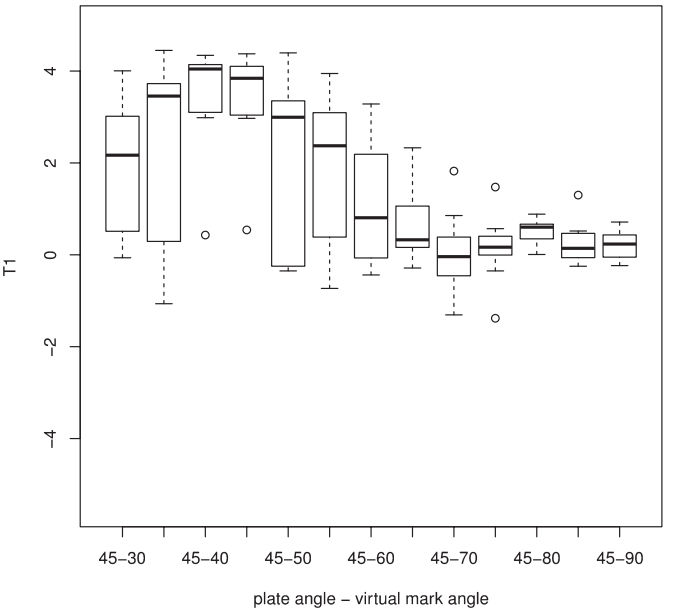

FIG. 16—*Averaged T1 values from statistical comparisons of 45° physical marks to virtual marks made with same side of the same tip.*

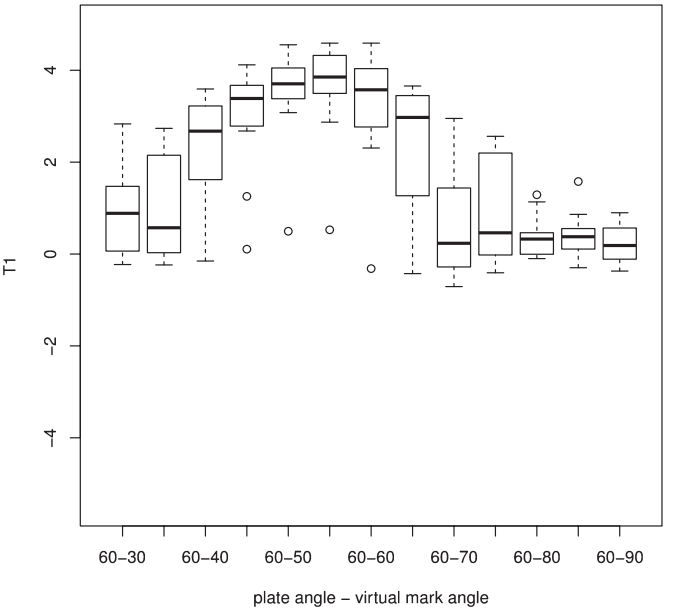

FIG. 17—*Averaged T1 values from statistical comparisons of 60° physical marks to virtual marks made with same side of the same tip.*

Performance Analysis

Based on these known match and known nonmatch results, a simple algorithm was designed to detect matches and infer their angle. A comparison set was defined as the results of comparing a certain marked plate to the virtual marks (30°, 35°, 40°, …, 85°, 90°) from a certain side of a certain tip. The maximum T1 value was found for each set in the results. If this T1 value was greater than 2.5, the comparison set was recorded as a match and the angle at which this T1 value was produced was recorded as the angle of the mark. Every match recorded by this algorithm was confirmed to be a true match, and only two known

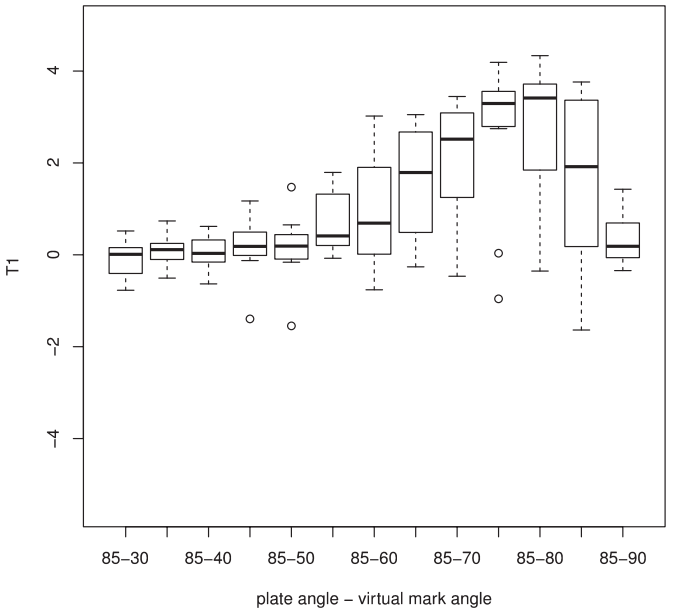

FIG. 18—*Averaged T1 values from statistical comparisons of 85° physical marks to virtual marks made with same side of the same tip.*

FIG. 19—*Comparison of 2D plate textures. (a) P8A-45. (b) P5A-45. (c) P2A-85.*

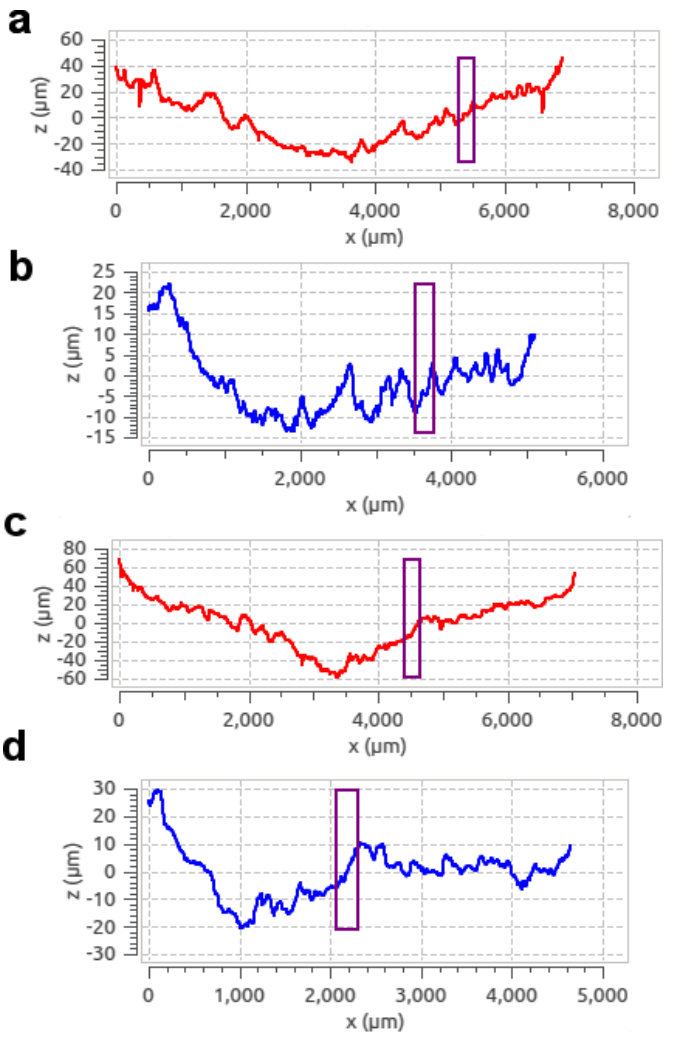

FIG. 20—*Suspected partial markings. (a) Virtual mark at 45° from Tip 5A. (b) Physical mark P5A-45. (c) Virtual mark at 85° from Tip 2A. (d) Physical mark P2A-85.*

matches were missed using this strategy (P5A-45 and P2A-85, as mentioned above).

Two potential reasons for the two false nonmatches have been identified. Figure 19 shows the 2D textures for P8A-45 (which was correctly matched) as compared to P5A-45 and P2A-85. Oxidation has left a large red rust spot on P5A-45. Moreover, oxidation has changed the reflectivity of P2A-85, making the plate difficult to image correctly. P2A-85 appears with more dark regions than the others. Therefore, oxidation may have changed the mark or contributed to increased imaging noise that caused a false nonmatch.

Moreover, visual inspection suggests that P5A-45 and P2A-85 may be partial markings. Figure 20 presents comparisons of the known matching virtual mark profiles to cross-sections from plates P5A-45 and P2A-85. In this figure, both physical marks appear to contain only about 60% of the full geometry of their respective tips. Comparisons of the plate textures before and after plate cleaning confirm that the cleaned plates contain the full set of striations recorded on the lead surface. Therefore, it is possible that these marked plates do not contain enough tip geometry for the current algorithm to consistently match them to the virtual marks.

Table 1 summarizes the error between the algorithmic prediction of the mark angle for the identified matches and the true mark angle. The median error for any true mark angle is −5°, and the average mark error is increasingly negative as the screwdriver handle approaches vertical. The virtual mark simulation is capable of positioning the cleaned tip geometry within floating point error, which is *c.* 1.2×10^{-5}%. Therefore, the likely sources of this error are slight variations in the T1 values produced for a given comparison and positioning error in the physical mark-making jig. For a given virtual and physical mark pair, the averaged T1 value was found to vary by about ±0.15 from comparison to comparison. This is to be expected based upon the random selection of window positions used for verification in the statistical algorithm of (3). This slight fluctuation is enough to have shifted the maximum T1 value by 5° for many of the comparison sets but not enough to influence the identification of matches. Moreover, as this fluctuation is random, it explains the random angle errors (such as the maximum error of 10° found for the 45° plates) far better than the systematic error in the means and medians. A better explanation for the systematic

TABLE 1—*Error (°) between the predicted angle of an identified match and the true angle.*

Statistic	45° Plates	60° Plates	85° Plates	Total
Mean	−1.667°	−4.583°	−6.364°	−4.375°
Median	−5°	−5°	−5°	−5°
Min	−10°	−10°	−10°	−10°
Max	10°	5°	0°	10°

angle error was found when examining the mark-making jig shown in Fig. 1. A slop of about 1° was discovered in the four-screw pattern, and a slop of 2–5° was discovered between the screwdriver bit and the holder. Both of these would cause the screwdriver tip to rotate slightly about the negative *y*-axis when pulling force is applied to the handle to make the mark. Moreover, as more force is required to make the marks as the screwdriver handle approaches vertical, this slop may also explain the trend of increasingly negative mean angle errors.

Despite these error sources, the algorithm could correctly predict the angle of the identified matches within ±5–10°. This agrees with the conclusion of tool mark examiners that marks from the same side of the same tool will match if they were made at angles within 15° of each other.

Conclusions

This study has introduced and investigated a new tool mark analysis approach that seeks to establish a more direct link between a tool and its mark. Both sides of six screwdriver tips were used to generate 34 marks on lead plates at angles to the horizontal of 45°, 60°, and 85°. Both the tips and the plates were digitized, and virtual marks generated from the tip geometry were compared to plate cross-sections using the statistical algorithm of (3). Using a simple analysis of the likelihood values, matches were identified with zero false positives and two false negatives. Moreover, the approach could determine the correct angle of the matched marks within ±5–10°. Although a weakness was identified in the statistical algorithm, it was not the fault of the virtual mark approach and did not affect the results of this preliminary study. However, the two false negatives suggest that partial marking phenomena may need to be incorporated into the simulation for future research.

These results, although preliminary, support existing conclusions of the forensics tool mark analysis community and hold potential both for reducing damage to the tool and for streamlining an examiner's workflow. The outcomes of this study support the conclusions that each side of each screwdriver makes its own unique marks and that these marks vary significantly with the angle of the screwdriver. Moreover, the success of the virtual marking simulation suggests that tip geometry is faithfully transferred to the lead plate during marking, and therefore, the potential exists to link a mark directly to a tool. The comparison of mark directly to tool geometry reduces the population under study from all marks to all tool tips, increasing the possibility of establishing reliable error estimates for the analysis. Finally, the optical profilometer does not alter the tip in any way during digitization, and the software can prepare the digitized geometry within minutes and generate and compare virtual marks within seconds. Therefore, this approach could quickly narrow down the range of possible angles for the examiner, allowing him or her to make and compare fewer physical marks. This would save time and reduce the potential damage to the tool tip. Moreover, given the speed of the software, it could potentially form the basis for a database of searchable virtual marks and physical marks.

Future research will seek to confirm these results on a larger set of tools and media. Moreover, potential modifications to the statistical algorithm to reduce or eliminate the weakness will be investigated.

Acknowledgments

The authors would like to express special thanks to Dr. Max Morris and Ms. Amy Hoeksema of the Iowa State University Statistics Department for their advice on integrating the statistical algorithm into the software and their guidance in analyzing and summarizing the results.

References

1. Petraco NDK, Shenkin P, Speir J, Diaczuk P, Pizzola PA, Gambino C, et al. Addressing the National Academy of Sciences' challenge: a method for statistical pattern comparison of striated tool marks. J Forensic Sci 2012;57(4):900–11.
2. Bachrach B. Development of a 3D-based automated firearms evidence comparison system. J Forensic Sci 2002;47(6):1–12.
3. Chumbley LS, Morris MD, Kreiser MJ, Fisher C, Craft J, Genalo LJ, et al. Validation of tool mark comparisons obtained using a quantitative, comparative, statistical algorithm. J Forensic Sci 2010;55(4):953–61.
4. Bolton-King RS, Bencsik M, Evans JPO, Smith CL, Allsop DF, Painter JD, et al. Numerical classification of curvilinear structures for the identification of pistol barrels. Forensic Sci Int 2012;220:197–209.
5. Geradts Z, Zaal D, Hardy H, Lelieveld J, Keereweer I, Bijhold J. Pilot investigation of automatic comparison of striation marks with structured light. In: Rudin LI, Bramble SK, Carapezza EM, editors. Enabling technologies for law enforcement and security. Proceedings of SPIE 4232. Boston, MA: SPIE, 2000;49–56.
6. Alicona Imaging GmbH. Focus variation. English edition, 2012; issuu.com/alicona/docs/alicona_focusvariation3_e_high_resolution (accessed May 21, 2013).
7. Bolton-King RS, Evans JPO, Smith CL, Painter JD, Allsop DF, Cranton WM. What are the prospects of 3D profiling systems applied to firearms and toolmark identification? AFTE J 2010;42(1):23–33.
8. Kidd JA. Comparison of screwdriver tips to the resultant toolmarks [master's thesis]. Ames, IA: Iowa State Univ, 2007.
9. Owens JD, Luebke D, Govindaraju N, Harris M, Krüger J, Lefohn AE, et al. A survey of general-purpose computation on graphics hardware. Comput Graph Forum 2007;26(1):80–113.
10. Zhang S, Ekstrand L, Grieve T, Eisenmann DJ, Chumbley LS. 3D data processing with advanced computer graphics tools. In: Schmit J; Creath K; Towers C.E, editors, Interferometry XVI: techniques and analysis. Proceedings of SPIE 8493. Bellingham, WA: SPIE, 2012;849310–7.

Additional information and reprint requests:
Song Zhang, Ph.D.
Mechanical Engineering Department
Iowa State University
2096 Black Engineering
Ames IA 50011
E-mail: song@iastate.edu